Avoided level crossings, diabolic points, and branch points in the complex plane in an open double quantum dot

I. Rotter[1,*] and A. F. Sadreev[2,3,4,†]
[1]*Max-Planck-Institut für Physik Komplexer Systeme, D-01187 Dresden, Germany*
[2]*Kirensky Institute of Physics, 660036, Krasnoyarsk, Russia*
[3]*Department of Physics and Measurement, Technology Linköping University, S-581 83 Linköping, Sweden*
[4]*Astafev Krasnoyarsk Pedagogical University, 660049 Krasnoyarsk, Russia*
(Received 27 July 2004; published 31 March 2005)

We study the spectrum of an open double quantum dot as a function of different system parameters in order to receive information on the geometric phases of branch points in the complex plane (BPCP). We relate them to the geometrical phases of the diabolic points (DPs) of the corresponding closed system. The double dot consists of two single dots and a wire connecting them. The two dots and the wire are represented by only a single state each. The spectroscopic values follow from the eigenvalues and eigenfunctions of the Hamiltonian describing the double dot system. They are real when the system is closed, and complex when the system is opened by attaching leads to it. The discrete states as well as the narrow resonance states avoid crossing. The DPs are points within the avoided level crossing scenario of discrete states. At the BPCP, width bifurcation occurs. Here, different Riemann sheets evolve and the levels do not cross anymore. The BPCP are physically meaningful. The DPs are unfolded into two BPCP with different chirality when the system is opened. The geometric phase that arises by encircling the DP in the real plane, is different from the phase that appears by encircling the BPCP. This is found to be true even for a weakly opened system and the two BPCP into which the DP is unfolded.

DOI: 10.1103/PhysRevE.71.036227 PACS number(s): 05.45.Mt, 03.65.Yz, 72.10.Bg, 03.65.Nk

I. INTRODUCTION

The phenomenon of avoided level crossing is studied theoretically as well as experimentally for many years. It is called also Landau-Zener effect or anticrossing of levels. This phenomenon is a general property of the discrete states of a quantum system: the energies of the states will never cross when the interaction between them is nonvanishing. Instead, their wave functions are exchanged at the critical value of a certain tuning parameter at which the avoided crossing takes place. The reason for the avoided crossing of two discrete levels follows from the expression for the two eigenvalues $e_\pm$ of the Hamiltonian of the system

$$e_\pm = \frac{e_1 + e_2}{2} \pm \frac{1}{2}\sqrt{(e_1 - e_2)^2 + 4\omega^2}, \tag{1}$$

where e_1 and e_2 are the diagonal elements of the symmetric Hamiltonian matrix while the ω are its nondiagonal elements. The e_1 and e_2 are the energies of the noninteracting states and ω is their interaction. Since the square root contains only positive values, e_+ and e_- are always different from one another with the only exception of vanishing interaction ω and $e_1 = e_2$.

It has been known for about 40 years [1] that the Hilbert space is incomplete when two discrete levels cross. Suppose, the identity $e_+ = e_-$ of the two eigenvalues of the Hamiltonian is not caused by any selection rule or symmetry property of the system and the eigenfunctions $\phi_\pm$ are well defined also at the crossing point. Then it follows that not only the eigenvalues $e_\pm$ but also the eigenfunctions $\phi_\pm$ of the Hamiltonian of the system are the same at the point of coalesced eigenvalues [1]. That means, the two eigenfunctions $\phi_\pm$ are linearly dependent and the spectrum is incomplete. This result is called "defect" of the Hilbert space, and the point where $\omega = 0$ and the two eigenvalues $e_\pm$ coalesce is called "exceptional point."

Another property related to avoided level crossings is the Berry phase [2,3]. It appears when a diabolic point (DP) is encircled: the phases of the two wave functions are not restored after one encircling, but are changed by π. Only the second encircling restores the wave functions including their phases. The Berry phase is of geometrical origin, and its existence is proven in many different experimental studies, e.g., Ref. [4]. It is proven experimentally also in a microwave cavity [5] where the phase change is traced in encircling a DP.

Equation (1) shows immediately that, in contrast to two discrete states, two resonance states may cross in the complex plane also when $\omega \neq 0$. The main reason is that the energies of resonance states are complex in contrast to the energies of discrete states which are real. The imaginary part of $e_{1,2}$ is the width (inverse finite lifetime) of the resonance state when isolated. Furthermore, also the interaction ω of resonance states may be complex due to the contributions originating from the coupling of the resonance states via the continuum [6]. The crossing point is a branch point in the complex plane (BPCP) [6–10]. Here, not only the real parts of $e_\pm$ coalesce but also their imaginary parts.

The resonance states are eigenstates of a nonhermitian Hamilton operator that describes the quantum system when

*Email address: rotter@mpipks-dresden.mpg.de
†Email address: almsa@ifm.liu.se; almas@tnp.krasn.ru

opened by embedding it into the continuum of input and output channels (continuum of scattering wave functions). The open quantum system is a subsystem of the total system containing both discrete and scattering states. The Hamiltonian of the open system consists of the hermitian Hamilton operator of the closed system with discrete states and the nonhermitian coupling term between discrete and scattering states [6,11]. Due to this coupling term, the discrete states of the closed system turn over into resonance states of the open system [12]. There is a $1 \leftrightarrow 1$ correspondence between the discrete states embedded in the continuum and the resonance states (for details see Ref. [6]).

A difference between discrete and resonance states is the normalization of the wave functions. While the wave functions of the discrete states are orthonormalized in the standard manner, the wave functions of the resonance states are biorthogonal [6,7,13,14] due to the nonhermiticity of the Hamilton operator describing the open quantum system. The components of the wave functions of resonance states diverge when a BPCP is approached [6,10,13,14]. Therefore, the wave functions of the two crossing resonance states cannot be considered as linearly dependent in spite of the relation $\psi_1 = \pm i\psi_2$ [6,8,10,15] holding between them at the singular point. This relation is rather an expression for nonlinear effects appearing at the BPCP [6,8,9]. Also the normalization and orthogonality of the wave functions are not in contradiction with one another at the BPCP since the difference between two infinitely large numbers may be zero or one [6,8,10]. The spectrum is therefore complete also at the BPCP [12].

Physically, the BPCP separate the regime of avoided level crossings from that without any crossing [6,10]. Characteristic of the states in the regime of avoided level crossing is the fact that their lifetimes are of comparable value. At the BPCP, however, the widths bifurcate [6,8,10,13–16]. As a consequence, the lifetimes of the states become different from one another, and there is no common time at which the states could cross or avoid crossing. Only in the projection onto the real energy axis, the resonance states cross.

Recently, the topology of a BPCP is studied theoretically as well as experimentally [17–22] by encircling it. As a result of these studies, the wave functions of the resonance states are restored only after four encirclings.

Furthermore, approaching a BPCP by varying the coupling strength v between system and environment is studied both theoretically and experimentally [19,22,23]. The BPCP has some chirality that is caused, obviously, by the fact that $\psi_1 \rightarrow \pm i\psi_2$ holds when the BPCP is approached [9]. Here, the wave functions can be written, e.g., as $\phi_{c1} = \sqrt{\frac{1}{2}}(\psi_1 \pm i\psi_2)$ and $\phi_{c2} = \sqrt{\frac{1}{2}}(\psi_2 \mp i\psi_1)$, respectively. The relative sign between the two wave functions determines the chirality.

The question arises whether or not there is a relation between the phases observed in encircling a BPCP and the Berry phase appearing in encircling a DP. Although this question is studied in different papers [21,24,25], a unique answer has not been found up to now. In Ref. [24], the phase in encircling the crossing point of two Gamow states differs from the usual Berry phase by an additional term that vanishes with vanishing width of the Gamow state. In Ref. [25], the relation $\psi_1 \rightarrow \pm i\psi_2$ holding in the very neighborhood of a BPCP, is used when encircling it. The unfolding of a DP into two different BPCP with different sign of the coupling strength v between system and environment, as suggested in Ref. [21], will surely take place. According to this suggestion, the encircling of the two different BPCP with different sign of v is expected to give the Berry phase [21]. This is, however, not the case [20,22]. The conclusion might be that still other features play a role when the two BPCP with different sign of v are encircled.

Double quantum dots (QDs) connected by a wire represent a very powerful example for a study of the relation between DPs and BPCP since they involve parameters of different type that can be controlled. There are not only parameters controlling the internal properties of the closed QD, which may be used for a study of the Berry phase. There are also parameters by means of which the coupling strength between the closed dot and the attached leads (environment of the dot) can be controlled. It is possible therefore to study the unfolding of a DP into the two BPCP with different sign of v when the system is embedded in the continuum.

In the following, we study the relation between DPs and BPCP in detail by using a double QD as an example. The basic equations and notations are given in Ref. [10] to which we refer directly in the present paper {e.g., Eq. (9) [10] means Eq. (9) of Ref. [10]}. Most important for the topic of the present paper are the eigenvalues and eigenfunctions of the hermitian Hamilton operator of the closed double dot system as well as those of the nonhermitian effective Hamilton operator that describes the system when opened by attaching leads to it. The surfaces in the four-manifold parameter space which define the BPCP, are shown in Sec. II. In Sec. III, the neighborhood of a BPCP is studied by approaching it by varying different parameters. The DPs and BPCP are studied by encircling them in Sec. IV. According to the analytical and numerical results, the DPs in the real plane and the BPCP have a completely different topological structure.

In Secs. V and VI, the BPCP and the DPs are encircled in the space of physical parameters. While the wave functions of the closed system are restored after two cycles around the DP, those of the open system are restored only after four cycles around the BPCP. This difference is caused by the fact that the eigenstates of the closed system are exchanged twice during one cycle while those of the open system are exchanged only once during one cycle. The exchange occurs, in any case, at an avoided level crossing appearing on the path of encircling the singular point. In Sec. VII, the relevance of the singular points for physical processes is discussed. At the BPCP, different Riemann sheets evolve. Their influence on physical observables can be seen in a large neighborhood.

II. THE BRANCH POINTS IN THE COMPLEX ENERGY PLANE

We consider BPCP in the case of a double QD that consists of two single dots coupled to each other by a wire (Fig. 1). The S matrix theory for transmission through such a QD

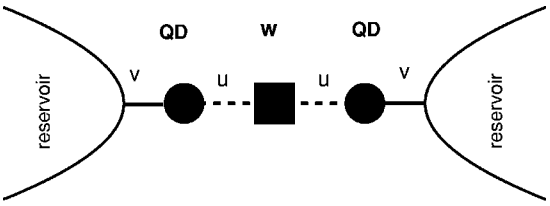

FIG. 1. Two single state QDs are connected to the wire w of length L with the coupling constants u and to the continuum of scattering wave functions ("reservoir") with the coupling constants v. The energy of the mode in the wire is $\epsilon(L)$ and those of the two single dots are ε_1^R and ε_1^L, respectively. Mostly the two single dots are assumed to be equal: $\varepsilon_1^R=\varepsilon_1^L\equiv\varepsilon_1$.

can be formulated by using the nonhermitian effective Hamilton operator that appears in the framework of the Feshbach projection operator technique [11]. The effective Hamilton operator for QDs in the tight-binding approach is derived in Refs. [26,27]. It contains the spectroscopic properties of the closed QD as well as the coupling matrix elements between the dot and the two attached leads. In the subspace of discrete states, the effective Hamilton operator has the general form

$$H_{\text{eff}} = H_B + \sum_{C=L,R} V_{BC}\frac{1}{E^+ - H_C}V_{CB}, \tag{2}$$

where H_B is the Hamiltonian of the closed double dot system and H_C is the Hamiltonian of the left ($C=L$) and right ($C=R$) reservoir and $E^+=E+i0$. The matrix elements of H_{eff} are calculated in the basis of the eigenstates of H_B, i.e., in a basis where H_B is *diagonalized* [6,16]. The second term of H_{eff} takes into account the coupling of the eigenstates of H_B via the reservoirs (continuum of incoming and outgoing waves) when the system is opened. The corresponding coupling matrix elements are denoted by V_{BC} and V_{CB}, respectively.

The equations that describe the double QD shown in Fig. 1, can be found in Refs. [10,27]. The energy of the single-channel transmission is related to the wave number by $E=-2\cos k$ [26]. Such a band gives rise to k-dependent coupling matrix elements in the effective Hamiltonian. By this k dependence, our model differs from the standard S matrix theory formulated in, e.g., Refs. [28,29].

We restrict the consideration to the case with only one state with energy ε_1 in each single dot, one mode ϵ propagating in the wire, and one channel (scattering wave function) in each of the two attached leads. For illustration, we consider ϵ as a linear function of the length L of the wire. This dependence of L may be replaced by a dependence on, e.g., the diameter of the wire without any influence on the discussion of the physical results. For simplicity, the coupling of the two single dots to the internal wire, denoted by u, is assumed to be the same for the two single dots. Also the coupling strength v between the whole double dot and the attached leads is taken to be the same for both leads.

The two eigenvalues $z_{1,3}$ of H_{eff}:

$$z_{1,3} = \frac{\varepsilon_1 + \epsilon(L) - v^2 e^{ik}}{2} \mp \sqrt{F}, \tag{3}$$

differ by $2\sqrt{F}$ where

$$F = \left(\frac{v^2 e^{ik}}{2} - \Delta\varepsilon\right)^2 + 2u^2 = \xi^2, \tag{4}$$

[see Eqs. (8) [10] and (16) [10]]. The point at which $F=0$, is a BPCP [6–8]. The two equations for the BPCP take the following form:

$$\Delta\varepsilon(L_c) = \frac{1}{2}v_c^2\cos k_c = -\frac{v_c^2}{4}E_c, \tag{5}$$

$$2u_c^2 = \frac{v_c^4}{4}\left(1 - \frac{E_c^2}{4}\right), \tag{6}$$

which define a surface of branch points for the four parameters of the system (see Fig. 2). For the energy at which the eigenvalues z_k coalesce, the fixed-point Eq. (14) [10] can be easily solved analytically. We obtain

$$E_c = E_k = \epsilon(L_c) = -\frac{4\Delta\varepsilon(L_c)}{v_c^2} \tag{7}$$

and

$$u_c^2 = \frac{\Delta\varepsilon(L_c)^2}{2}\left[\frac{4}{\epsilon(L_c)^2} - 1\right]. \tag{8}$$

These conditions reduce the number of physical parameters from four to three, v_c, u_c, L_c, related to one other by two equations.

We underline that the coalescence of two eigenvalues of H_{eff} at a certain energy E of the system does not mean that also two poles of the S matrix coalesce at this energy. The point is that the eigenvalues z_k of H_{eff} are energy dependent

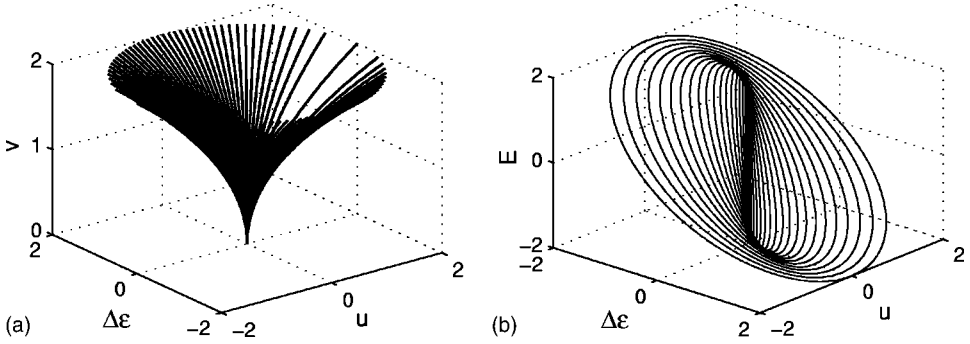

FIG. 2. The surfaces of the BPCP in the four-manifold parameter space $\Delta\varepsilon(L)\equiv(\varepsilon_1-\epsilon(L))/2, u, v, E$, defined by Eqs. (5) and (6).

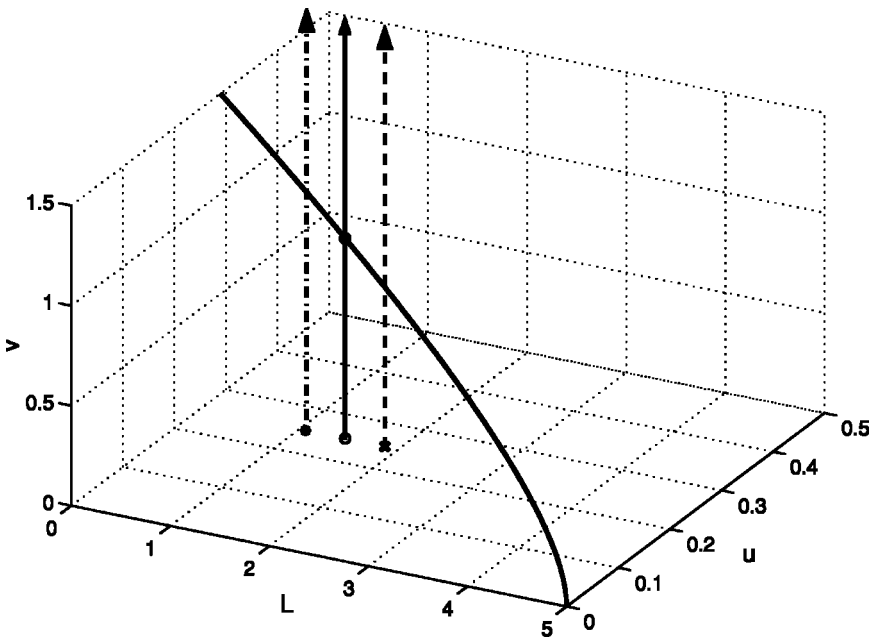

FIG. 3. The line of the BPCP in the three-manifold parameter space L, u, v (solid line). The three arrows show paths as a function of v (by keeping u and L constant) which start at $v=0$, $u=u_c$ and different L. The path starting at $L=L_c$ (shown by an open circle) crosses the line of the BPCP at $v=v_c$ (shown by a full circle). The paths which start at $L=L_c\pm\Delta L$ (shown by a star and a cross, respectively) do not cross the line of the BPCP.

functions. Only the solutions of the fixed-point equations, $E_k=\mathrm{Re}(z_k)|_{E=E_k}$, and the widths defined by $\Gamma_k=-2\,\mathrm{Im}(z_k)|_{E=E_k}$ are numbers that correspond [30] to the poles of the S matrix. In the general case, the two levels whose (energy dependent) eigenvalues coalesce at the energy $E=E_c$, avoid crossing.

III. APPROACHING BRANCH POINTS IN THE COMPLEX PLANE

Here, we are interested in the question how the eigenvalues z_k, Eq. (3), and eigenvectors $|k)$, Eq. (9) [10], of the effective Hamiltonian H_{eff} behave when we trace them along a certain line that touches the surface of BPCP as it is shown in Fig. 2(a). For a fixed energy E the BPCP surface reduces to the BPCP line shown in Fig. 3. If we start at $v=0$ [and $u=u_c$, $\Delta\varepsilon_c\equiv\Delta\varepsilon(L_c)$], the path will cross the line of the BPCP at $v=v_c$ shown in Fig. 3 by a full circle. At the BPCP line, the absolute values of the eigenvector components $|a|$, $|b|$ are singular and the phases of the components $\alpha=\arg(a)$, $\beta=\arg(b)$ are not determined. We can therefore not trace the path when crossing the BPCP line. We can choose, however, paths that cross the very neighborhood of the BPCP line. Two such paths are shown in Fig. 3 by the dashed and dot-dashed arrows.

The behavior of the eigenvalues and eigenvectors as a function of the coupling strength v along the two paths with $L=L_c\pm\Delta L$ is shown in Figs. 4 and 5. The parameters are chosen as $\varepsilon_1=1$, $\epsilon(L)=2-L/5$, $u=u_c$, $E=E_c$ but $L=L_c\pm0.01$. Here $L_c=1.4645$, $u_c=1/4$ and $E_c=\sqrt{2}$ are the critical physical parameters which define the BPCP line shown in Fig. 3 provided that $v=v_c=1$.

Let us consider at first the case $L=L_c-\Delta L$ shown in Fig. 4 where $\Delta L=0.01$ is small as compared to L_c. The real parts of z_1 and z_3 repel each other at $v<1$ and cross at $v=v_{c'}\approx v_c=1$. The imaginary parts of z_1 and z_3 are similar when $v<1$ but $|\mathrm{Im}(z_1)-\mathrm{Im}(z_3)|\neq0$ for all v, including the critical value. In the other case $L=L_c+\Delta L$, shown in Fig. 5, the real parts of z_1 and z_3 achieve a minimal distance when $v=v_{c''}\approx v_c$ but do not cross. The imaginary parts of z_1 and z_3, however, become equal at the critical value of v. The last scenario at $v<1$ is that of avoiding level crossing in the complex plane, see Refs. [9,10,16]. When $v>1$, the widths bifurcate in both cases. The wave functions are exchanged at the critical value of v in Fig. 5, but they are not exchanged in Fig. 4.

The two figures show further that also the complex amplitudes a and b of the eigenvector components, defined by Eqs. (9) [10] and (10) [10], have characteristic features at $v=v_{c'}$ $(v_{c''})$: $|a|\gg1$, $|b|\gg1$, and the phases $\alpha=\arg(a)$ and $\beta=\arg(b)$ jump by, respectively, $+\pi/4$ when $L=L_c+0.01$ (Fig. 5) and $-\pi/4$ when $L=L_c-0.01$ (Fig. 4). Note that the features observed in the amplitudes a and b at $v\approx v_c$ are the more pronounced the smaller ΔL is. According to (9) [10] and (10) [10], $|a|\to\infty$, $|b|\to\infty$, $v_{c'}(v_{c''})\to v_c$ when $\Delta L\to0$.

In Figs. 4 and 5, the phase jumps at $L=L_c\pm\Delta L$ are of different sign when traced as a function of increasing v. When traced, however, in one case as a function of increasing v and in the other case as a function of decreasing v, the two phase jumps add to $\pm\pi/2$. This last case corresponds to a connecting of the two paths with $L=L_c\pm\Delta L$ at $v=\pm\infty$, i.e., an encircling of the BPCP along a path that is very different from a circle. The encircling of a BPCP along different paths will be discussed in the next two sections. Here, we mention only that the phase jumps $\pi/2$ appearing when crossing the BPCP, are related to a change of the Riemann sheet.

Analog results are obtained when the evolution of the eigenvalues z_k and of the components a and b of the eigenfunctions of the effective Hamiltonian H_{eff} are considered as a function of another parameter. The parameter may even be the energy E of the system as shown in Fig. 6.

In Figs. 4–6, we traced the eigenvalues z_1 and z_3, Eq. (3), and eigenfunctions $|1)$ and $|3)$, Eq. (9) [10], of the effective Hamiltonian H_{eff} as a function of the coupling strength v

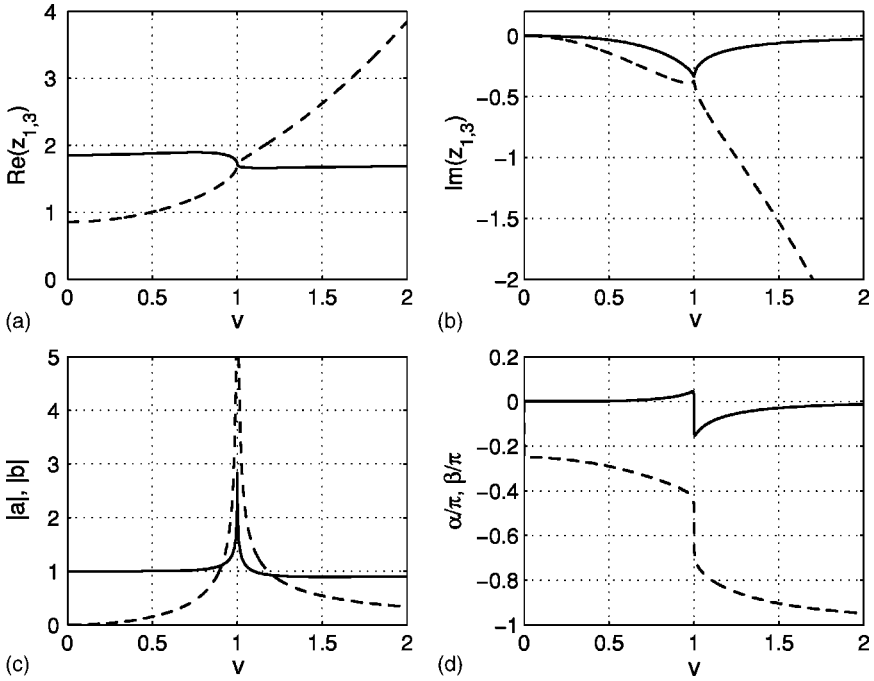

FIG. 4. The evolution of the eigenvalues z_1 (solid lines) and z_3 (dashed lines) (a, b) and of the components $a=|a|e^{i\alpha}$ (dashed lines) and $b=|b|e^{i\beta}$ (solid lines) of the eigenfunctions $|1\rangle$ and $|3\rangle$ (c, d) of the effective Hamiltonian H_{eff} as a function of v for $E=E_c=\sqrt{2}$. The parameters $u=u_c=1/4$, $L=L_c-0.01$, $L_c=1.4645$ correspond to the point shown in Fig. 3 at $v=0$ by a star. The evolution corresponds to the path shown in Fig. 3 by the dashed-dotted arrow. $\varepsilon_1=1$, $\epsilon(L)=2-L/5$. At the critical value of v, $|a|\gg 1$, $|b|\gg 1$ and the phases jump by $-\pi/4$.

>0. Analog pictures will be obtained for $v<0$ since only v^2 enters the basic equations.

Note further that, due to the strong energy dependence of the eigenvalues, there are two BPCP as a function of E: one at $L_{c_1}=1.4645$, $E_{c_1}=\sqrt{2}$ and the other one at $L_{c_2}=8.5355$, $E_{c_2}=-\sqrt{2}$. The two levels repel in energy, and the widths of the two states are comparable in value when $E>\sqrt{2}$ in the first case and $E<-\sqrt{2}$ in the second case. In this regime, the two levels avoid crossing in the complex plane. The jumps in the phases α and β have different sign at the two different BPCP when traced as a function of increasing E.

The two BPCP at $L_{c_1}=1.4645$, $E_{c_1}=\sqrt{2}$ and at $L_{c_2}=8.5355$, $E_{c_2}=-\sqrt{2}$ are an illustration of the fact that the BPCP do not coincide, generally, with a double pole of the S matrix [30], as stated in Sec. II. In both cases E_c is different from E_1 and E_3: $E_{c_1}=\sqrt{2}=1.41$ and $E_{c_2}=-\sqrt{2}=-1.41$ while $E_{1,3}=1.71$ in the first case and $E_{1,3}=0.29$ in the second case. The difference between $E_{1,3}$ and E_{c_1} is within the uncertainty determined by the widths of the two states ($\Gamma_{1,3}/2=0.35$). The other BPCP is, however, very distant as compared to the corresponding $\Gamma_{1,3}/2$. The influence of this BPCP on physical observables is therefore very limited.

At the BPCP the phases α,β are not determined. Every BPCP is a chiral state. The two BPCP corresponding to $v=1$ and $v=-1$ have different chirality (Figs. 4–6). The chiral-

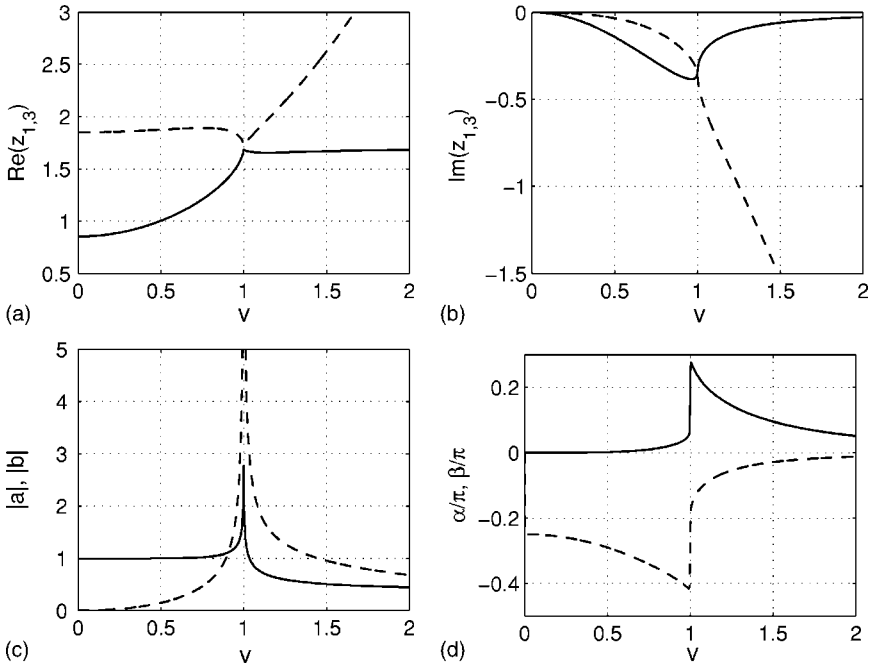

FIG. 5. The same as Fig. 4 but $L=L_c+0.01$. At $v=0$, the evolution starts at the point shown in Fig. 3 by a cross. The evolution corresponds to the path shown in Fig. 3 by the dashed arrow. At the critical value of v, it is $|a|\gg 1$, $|b|\gg 1$ and the phases jump by $+\pi/4$.

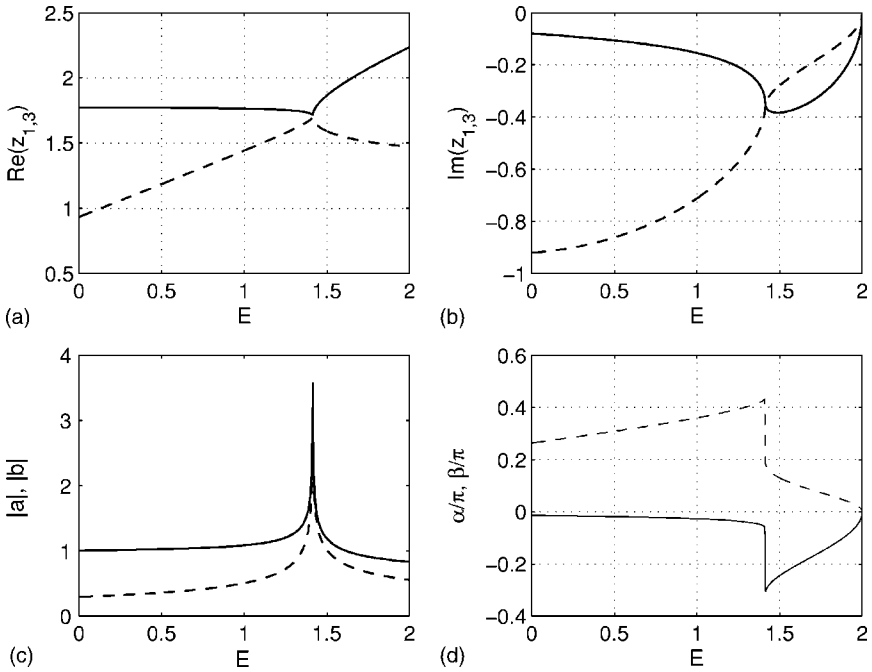

FIG. 6. The evolution of the eigenvalues z_1 (solid lines) and z_3 (dashed lines) (a, b) and of the components $a=|a|e^{i\alpha}$ (dashed lines) and $b=|b|e^{i\beta}$ (solid lines) of the eigenfunctions $|1\rangle$ and $|3\rangle$ (c, d) of the effective Hamiltonian H_{eff} as a function of E for $v\approx v_c=1$ ($v<v_c$). The other parameters of the system satisfy the Eqs. (5) and (6): $L=L_{c_1}=1.4645$, $u=u_c=1/4$, $\varepsilon_1=1$, $\epsilon(L)=2-L/5$. At the critical value of E, it is $|a|\gg 1$, $|b|\gg 1$ and the phases jump by $-\pi/4$.

ity of a BPCP has been studied experimentally by approaching it in a microwave cavity [19,22].

From Figs. 4–6, we conclude that the real and imaginary parts of the components of the wave functions evolve differently with v and E, respectively, in the regime of avoided level crossing. This result has an important influence on the transmission through QDs. An example is shown in Fig. 4 of Ref. [10] where the transmission is enhanced in the region where the phases α and β are approaching the phase jump. In this regime, the widths of the states are comparable in value and the states avoid crossing.

IV. ENCIRCLING BRANCH POINTS IN THE COMPLEX PLANE AND DIABOLIC POINTS IN THE REAL PLANE

Let us consider the two cases when

the real eigenvalues E_1^B and E_3^B of H_B coalesce and

the complex eigenvalues z_1 and z_3 of H_{eff} coalesce.

The first case is a DP while the second one is a BPCP. Both points with coalesced eigenvalues are related to avoided level crossings. According to (3) and (4), the condition for a BPCP to appear is $F=\xi^2=0$. The corresponding condition for a DP is $\eta=0$ with [10]:

$$\eta^2=\Delta\varepsilon^2+2u^2. \tag{9}$$

Discrete states of the double QD can cross therefore only when the interaction between the single QDs and the internal wire vanishes, $u=0$. In contrast to this, resonance states may cross, according to (4), also when the interaction between them is different from zero. This holds for the direct internal interaction u as well as for the external interaction v of the resonance states via the continuum of scattering wave functions which occurs due to their overlapping. The BPCP and DPs have therefore a completely different physical meaning.

We will show now that the DPs and BPCP are completely different also from a mathematical point of view. To this aim, we study the topological structure related to them.

The fundamental topological properties of certain points can be easily established by encircling them. Let us first analyze the DP, at which two (or three) real eigenvalues of the hermitian Hamilton operator H_B coalesce, independently of any symmetry relation for the system [3]. The properties of these points are well known. They are related to avoided crossings of discrete levels, and an encircling of them causes the well-known Berry phase [2].

The DP defined by $\eta=0$ is characterized, according to (9), by $u=0$, $\Delta\varepsilon=0$ in the real plane of the parameters u, $\Delta\varepsilon$ of the closed system. By encircling the DP according to

$$\Delta\varepsilon=\eta\cos\theta,\quad \sqrt{2}u=\eta\sin\theta, \tag{10}$$

we obtain that E_1^B and E_3^B vary as $\cos\theta$ and

$$|1\rangle=\frac{1}{\sqrt{2}}\begin{pmatrix}-\sin\theta/2\\ \sqrt{2}\cos\theta/2\\ -\sin\theta/2\end{pmatrix},\quad |3\rangle=\frac{1}{\sqrt{2}}\begin{pmatrix}\cos\theta/2\\ \sqrt{2}\sin\theta/2\\ \cos\theta/2\end{pmatrix}. \tag{11}$$

We see immediately that after each encircling of a DP, the eigenvalues of H_B are restored and the eigenfunctions change their sign. That means, the eigenstates of the closed system are restored after two cycles. Equations (11) express the well-known Berry phase in our model system.

Let us now consider the BPCP that appear in the open system when $F=\xi^2=0$, Eq. (4). They are given by Eqs. (5) and (6). Let us encircle the BPCP by defining $F=X+iY=R\exp(i\phi)$, $R=|F|$. Substituting these expressions into (4) gives

$$X=|F|\cos\phi=\eta^2+\frac{v^4}{4}\cos 2k-v^2\cos k\Delta\varepsilon,$$

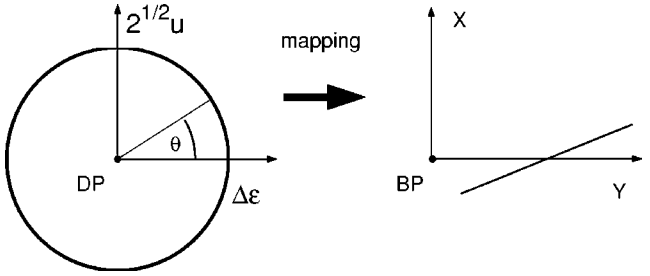

FIG. 7. The encircling of the diabolic point $u=0$, $\Delta\varepsilon=0$, given by Eq. (10), (left) and its mapping onto the plane X,Y (right) according to Eq. (13).

$$Y = |F|\sin\phi = \frac{v^4}{4}\sin 2k - v^2 \sin k\Delta\varepsilon. \tag{12}$$

We see that by encircling a BPCP, the eigenvalues z_k of the effective Hamiltonian H_{eff} behave as $z_1 - z_3 \sim \exp(i\phi/2)$ while the components of the eigenstates behave as $a,b \sim \exp(-i\phi/4)$. This result is similar to that found in Ref. [21]. It means that the eigenvalues of the effective Hamiltonian are restored after two cycles while the eigenstates are restored only after four cycles. Thus the DPs and the BPCP differ when encircled.

Now the following question arises. Can the encircling of the DP give rise to a nontrivial phase behavior of the eigenstates of H_{eff}? From (10) and (12) we obtain

$$X = r^2 + \frac{v^4}{4}\cos 2k - v^2 \cos k\, r \cos\theta,$$

$$Y = \frac{v^4}{4}\sin 2k - v^2 \sin k\, r \cos\theta, \tag{13}$$

where $r=\eta$. The mapping of the encircling of a DP in the plane $\Delta\varepsilon$, $\sqrt{2}u$ onto the complex plane X,Y is shown in Fig. 7. Irrespective of the choice of the parameters E and v of the open system, the encircling of the DP maps onto a straight line in the X,Y plane. It does not cross the branch point $X=0$, $Y=0$. Hence, the encircling of the DP has no consequence for the open system.

We will now consider the opposite case, i.e., we start from the encircling of the BPCP in the complex plane X,Y. Some simple algebra gives us, according to (13), the following mapping:

$$\Delta\varepsilon = -\frac{v^2}{4}E - \frac{Y}{v^2\sqrt{1-\frac{E^2}{4}}},$$

$$2u^2 = X + \frac{v^4}{4}\left(1-\frac{E^2}{4}\right) - \frac{Y^2}{v^2\left(1-\frac{E^2}{4}\right)}. \tag{14}$$

This mapping simplifies by choosing $E=0$:

$$\Delta\varepsilon = -\frac{Y}{v^2},$$

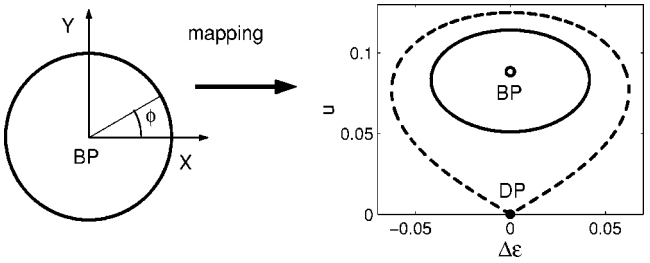

FIG. 8. The encircling of the branch point $X=0$, $Y=0$, given by Eq. (12), (left) and its mapping onto the plane $\Delta\varepsilon$, u (right) according to Eq. (15) for $E=0$, $v=0.5$. Dashed line: $R=v^4/4$, solid line: $R=v^4/6$. The point marked by an open circle corresponds to the branch point $X=0$, $Y=0$. The point marked by a full circle corresponds to the DP $\Delta\varepsilon=0$, $u=0$.

$$2u^2 = X + \frac{v^4}{4} - \frac{Y^2}{v^2}. \tag{15}$$

From these expressions, we obtain the condition $R \leqslant v^4/4$ for the encircling radius. The mapping (15) is shown in Fig. 8 by the dashed line for a fixed value of the coupling constant v. The case $E \neq 0$ shifts the mapping to the plane $\Delta\varepsilon$, u but never encircles the DP. Thus, irrespective of the choice of v and E, the encircling of the BPCP does not encircle the DP.

The conclusions from the two mappings shown in Figs. 7 and 8 are the following.

(i) The encircling of a DP gives rise to a geometric phase in the closed system, and does not cause any phase in the open system.

(ii) The encircling of the BPCP gives rise to a geometric phase in the open system but has no effect in the closed system.

V. ENCIRCLING A BPCP IN THE SPACE OF PHYSICAL PARAMETERS

The double QD considered by us in the foregoing sections consists of two identical single dots and a wire connecting them, Fig. 1. It is characterized by four physical parameters. The two parameters u and $\Delta\varepsilon(L)$ are defined in the closed system while the two parameters v and E are meaningful only in the open system. Using two of these four parameters for each encircling of a BPCP, we can realize six types of encircling. There are still other couples of parameters as, e.g., ε_1 and L. They are, however, dependent from one another at the BPCP, Eqs. (5) [10] and (5), and can therefore not be used for a meaningful encircling of a BPCP in our simple model system.

In microwave transmission it is comparably easy to vary the frequency and the length of the wire, i.e., to vary E and $\Delta\varepsilon(L)$. We begin therefore with the encircling of the BPCP by varying E and L, i.e., by varying the squared frequency of the microwave transmission and the length of the wire. The other parameters belonging to the branch point surface shown in Fig. 2, remain fixed ($v=1, u=1/4$). In this case, the encircling is given by

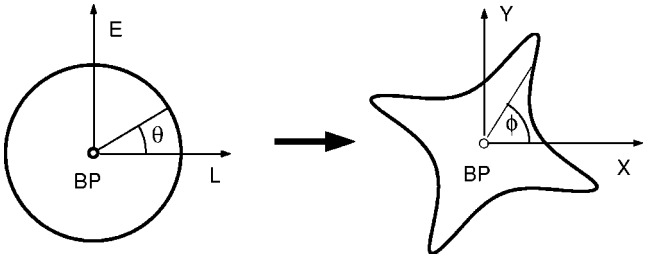

FIG. 9. Mapping of the encircling of the BPCP (open circle) in the plane $E=\sqrt{2}+r\sin\theta$, $L=1.4645+r\cos\theta$ onto the plane $X=R\cos\phi$, $Y=R\sin\phi$ given by Eq. (17) for $r=0.25$. $E_c=\sqrt{2}$, $L_c=1.4645$, $v=v_c=1$, $u=u_c=1/4$, $\varepsilon_1=1$, $\epsilon(L)=2-L/5$.

$$E = E_c + r\sin\theta, \quad L = L_c + r\cos\theta, \tag{16}$$

where $E_c=\sqrt{2}$, $L_c=5(1-1/\sqrt{2})=1.4645$. This encircling maps onto the complex plane (X,Y) in accordance to Eq. (12):

$$X = R\cos\phi = (\Delta\varepsilon(L)+E)^2 + \frac{E^2}{16} - \frac{1}{8},$$

$$Y = R\sin\phi = -\left(\Delta\varepsilon(L)+\frac{E}{4}\right)\sqrt{1-\frac{E^2}{4}}, \tag{17}$$

where E and L are given by (16). The mapping of the encircling (16) onto the encircling (17) is shown in Fig. 9. Although this mapping looks complicated, the encircling in the plane L, E gives rise to the encircling in the complex plane X, Y. The dependence of the eigenvalues and eigenfunctions, Eqs. (3) and (9) [10], respectively, of the effective Hamiltonian $H_{\rm eff}$ on the encircling angle θ is shown in Fig. 10.

In microwave transmission it is also possible to vary the coupling v of the leads to the billiard [31,32]. The encircling in the plane L, v is

$$L = L_c + r\cos\theta, \quad v = v_c + r\sin\theta. \tag{18}$$

The mapping of this encircling onto the complex plane X, Y is shown in Fig. 11. The circular encircling (18) gives rise to a very anisotropic encircling in the X, Y plane, see the dashed line in Fig. 11(b). The encircling of the BPCP becomes more isotropic when an elliptical encircling in the plane L, v is chosen, as shown by the solid lines in Fig. 11. The eigenvalues and eigenfunctions of the effective Hamiltonian $H_{\rm eff}$, Eqs. (3) and (9) [10], respectively, as a function of the encircling angle θ are shown in Fig. 12.

The eigenvalue pictures 10 and 12 show that in the space of the parameters L, E as well as L, v the two states 1 and 3 avoid crossing in the complex plane only once during each cycle: the avoided level crossing seen in the projection onto the real energy axis and accompanied by a "crossing" in the projection onto the imaginary width axis [more exactly: by $\mathrm{Im}(z_1)=\mathrm{Im}(z_3)$], takes place only once within one cycle. Another time, a crossing appears in the projection onto the real energy axis that is accompanied by $\mathrm{Im}(z_1)\neq\mathrm{Im}(z_3)$ (no crossing in the projection onto the imaginary width axis). This behavior proves once more that the crossing scenario changes at the BPCP. As a consequence, the two states are exchanged after one encircling and the eigenvalues are restored only after the second cycle. The moduli of the components of the wave functions have maxima in each cycle and repeat their behavior after every second encircling. The phases of the components of the eigenvectors are, however, restored only after four encirclings.

These results agree with those discussed in Secs. III and IV as well as in Refs. [17,21,22]. Above all, they agree with those obtained experimentally in a microwave cavity [18,20,22]. That means, the BPCP are of fourth order. It is clear from Eqs. (16) and (18) and from all the figures shown that the encircling of a BPCP in the opposite direction corresponds to the encircling of a BPCP with the opposite

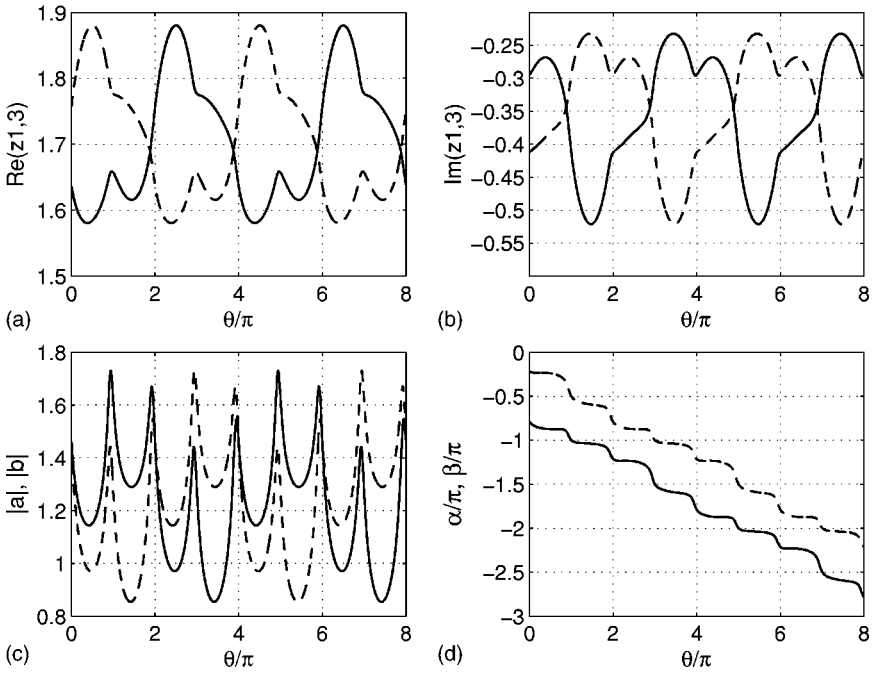

FIG. 10. The evolution of $\mathrm{Re}(z_k)$ (a) and $\mathrm{Im}(z_k)$ (b) of the two eigenvalues z_1 (solid lines) and z_3 (dashed lines) of the effective Hamiltonian $H_{\rm eff}$ as a function of the angle θ. The corresponding evolution of the components $a=|a|e^{i\alpha}$ (solid lines) and $b=|b|e^{i\beta}$ (dashed lines) of the two eigenvectors $|1\rangle$ and $|3\rangle$ (c, d). The encircling is around the BPCP in the plane E, L given by (16). The parameters are the same as in Fig. 9. The eigenvalues z_k and the moduli $|a|$, $|b|$ are restored after two cycles while the phases α, β are restored after four cycles.

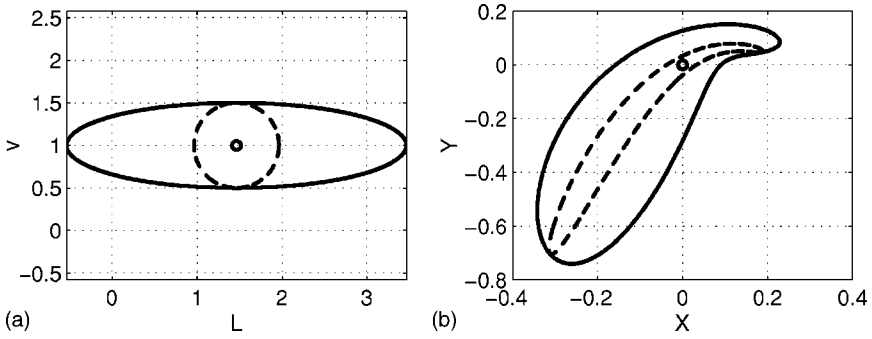

FIG. 11. Mapping of the circular encircling of the BPCP (open circle) in the plane $L=L_c+0.5\cos\theta$, $v=v_c+0.5\sin\theta$ (dashed line) and of the elliptic encircling $L=L_c+2\cos\theta$, $v=v_c+0.5\sin\theta$ (solid line) onto the plane $X=R\cos\phi$, $Y=R\sin\phi$ for $r=0.5$. It is $v=v_c=1$, $E=E_c=\sqrt{2}$, $L=L_c=1.4645$, $u=u_c=1/4$, $\varepsilon_1=1$, $\epsilon(L)=2-L/5$.

chirality. Also this result is in agreement with the experimental ones [18,20,22].

Similar pictures are obtained when other parameters are varied such as the energy ε_1 of the single dots or the coupling strength u of the two single dots to the internal wire. An exception is only the case when the two parameters considered are related to one another at the BPCP, as it is the case in our simple model for, e.g., the energy ε_1 of the single dot and the length L, Eqs. (5) [10] and (5).

The encircling of the two BPCP with $v=\pm1$ (and $E=E_{c_1}=\sqrt{2}$, $L=L_{c_1}=1.4645$, $u=u_v=1/4$) corresponds to an encircling of two BPCP that have different chirality. Therefore, the phase changes compensate each other. As a consequence the wave functions, including their phases, are restored after every encircling. The situation is another one when the two BPCP are encircled in opposite directions as discussed in Refs. [20,22]. Since the two BPCP are of the same type, the number of encirclings of a BPCP is simply doubled in such a procedure. Accordingly, the phases of the wave functions are restored already after two encirclings of both BPCP. A similar picture follows when the two BPCP $E_{c_2}=-\sqrt{2}$, $L_{c2}=8.5355$ at $v=\pm1$ are encircled.

VI. ENCIRCLING A DP IN THE SPACE OF PHYSICAL PARAMETERS

We consider now the evolution of the eigenvalues E_k^B, Eq. (4) [10], and eigenvectors $|k\rangle$, Eq. (6) [10], of the Hamiltonian H_B by encircling of a DP in the space of physical parameters of the closed double QD. The parameters varied are the length L of the wire and the internal coupling strength u. The other parameters [$\epsilon(L)=2-L/5$ for the energy of the wire and $\varepsilon_1=1$ for the energy of the single dots] are the same as in Fig. 4, but $v=0$. The circular encircling of the DP is

$$L=5+10r\cos\theta,\quad u=\frac{r}{\sqrt{2}}\sin\theta \tag{19}$$

according to (10) with $r=\eta$, while an elliptic encircling is given, e.g., by

$$L=5+0.25\cos\theta,\quad u=0.1\sin\theta. \tag{20}$$

For the circular encircling, the difference between the eigenvalues does not depend on θ according to (9), and the evolution of the eigenvectors of H_B is given by (11). The results of the elliptic encircling (20) are shown in Fig. 13.

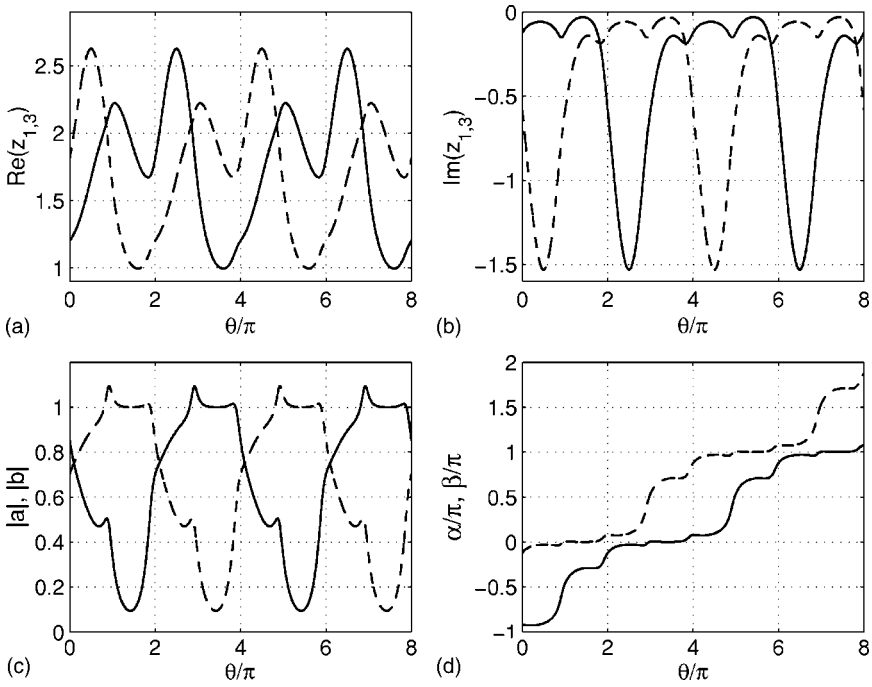

FIG. 12. The evolution of $\mathrm{Re}(z_k)$ (a) and $\mathrm{Im}(z_k)$ (b) of the two eigenvalues z_1 (solid lines) and z_3 (dashed lines) of the effective Hamiltonian H_{eff} as a function of the angle θ. The corresponding evolution of the components $a=|a|e^{i\alpha}$ (solid lines) and $b=|b|e^{i\beta}$ (dashed lines) of the two eigenvectors $|1\rangle$ and $|3\rangle$ (c, d). The elliptical encircling is around the BPCP in the plane L, v shown in Fig. 11 by the solid lines. The parameters are the same as in Fig. 11. The eigenvalues z_k and the moduli $|a|$, $|b|$ are restored after two cycles while the phases α, β are restored after four cycles.

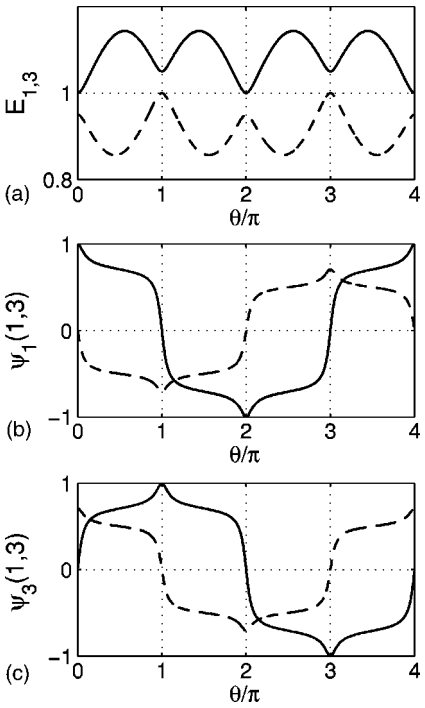

FIG. 13. The evolution of the two eigenvalues $E^B_{1,3}$, Eq. (4) [10], (a) and eigenvectors $\psi_m(k)$, m, $k=1,3$, Eq. (6) [10], (b, c) of the Hamiltonian H_B of the closed system for the elliptic encircling $L=5+0.25\cos\theta$, $u=0.1\sin\theta$. E_1 is shown in (a) by the solid line and E_3 by the dashed line. The components $\psi_1(1)$, $\psi_3(1)$ are shown by the dashed lines in (b, c), and the components $\psi_1(3)$, $\psi_3(3)$ by the solid lines. The eigenvalues are restored after every cycle while the eigenvectors are restored after two cycles.

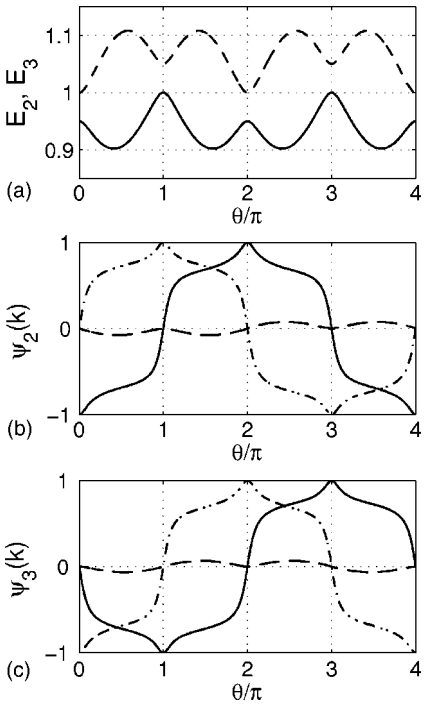

FIG. 14. The same as Fig. 13 but for a double QD consisting of two different single QDs with $\varepsilon^L_1=1$, $\varepsilon^R_1=0$, and a wire of length L. E_2 is shown in (a) by the solid line, E_3 by the dashed line. In (b, c), the components $\psi_m(k)$, $m=2,3$, $k=1,2,3$ are shown. Dotted-dashed line: $k=1$, solid line: $k=2$ and dashed line: $k=3$. The eigenvalues are restored after every cycle while the eigenvectors are restored after two cycles.

According to (9) and (4) [10] and (5) [10], all three eigenvalues E^B_k coalesce at the DP ($\eta=0$) when the two single QDs are identical. For comparison, we show therefore in Fig. 14 the results obtained for the elliptical encircling (20) when only two eigenvalues coalesce. Here, the two single dots are different from one another, i.e., ε^L_1 of the left dot is different from ε^R_1 of the right dot.

Common to all types of encircling is the following. During each cycle of θ, the internal interaction u vanishes twice. Each time, the two states avoid crossing and the two wave functions $|1\rangle$ and $|3\rangle$ are exchanged according to (6) [10]. As a consequence, the two eigenvalues are restored after each cycle, and the eigenvectors are restored only after two cycles. This result is in full correspondence to those obtained by Berry [2] and with Eq. (11) for the circular encircling. It differs, however, from the results obtained from an encircling of the BPCP (Sec. V) where an avoided level crossing appears only once in each cycle and the two eigenvalues are restored therefore only after two encircling cycles.

In Fig. 13, some internal symmetry of the system is involved in the results which arises from the identity of the two single dots. We underline, however, that the system as a whole does not show any symmetry due to the wire that connects the two single dots in an unsymmetrical manner. The results shown in Fig. 13 should be compared (qualitatively) with the experimental results obtained in the case of three crossing states of a rectangular microwave billiard [5]. In these data, a phase change was observed that arises, according to the authors of Ref. [5], from an additional mirror symmetry in the system. Meanwhile, this symmetry is explained as being due to off-diagonal Berry phases [33]. It seems to be that the phase changes observed in the two different cases are of the same origin.

We study now the influence of extending the function space by including scattering states. In Figs. 15 and 16, we show the evolution of the eigenvalues z_k and of the components a and b of the eigenvectors of the effective Hamiltonian $H_{\rm eff}$ by using the parameters (19) and (20) for, respectively, circular and elliptic encircling of a DP but allow for a nonvanishing coupling strength v to the continuum. The real parts $\mathrm{Re}(z_k)$ of the eigenvalues of the effective Hamiltonian $H_{\rm eff}$ show the same behavior as the eigenvalues E^B_k of the Hamiltonian H_B, see Eqs. (4) [10], (10) for the circular encircling, and Fig. 13(a) for the elliptical encircling of the DP. The similarity is the larger the smaller v is. The widths of the two resonance states, which do not have any counterpart in the closed system, are strongly dependent on θ. The wave functions of the two resonance states reflect the biorthogonality relations $(z_k|z_l)=\delta_{k,l}$. As can be seen from the two Figs. 15 and 16, the amplitudes of a and b are no longer restricted by the standard normalization condition $|\psi_k|^2=1$. The wave functions are normalized to $(\psi_k)^2=1$, and $|\psi_k|^2$ may be larger than one. In our calculations, $|a|=1$, $|b|=0$ (or $|a|=0$, $|b|=1$) only when the path passes $u=0$. The structure

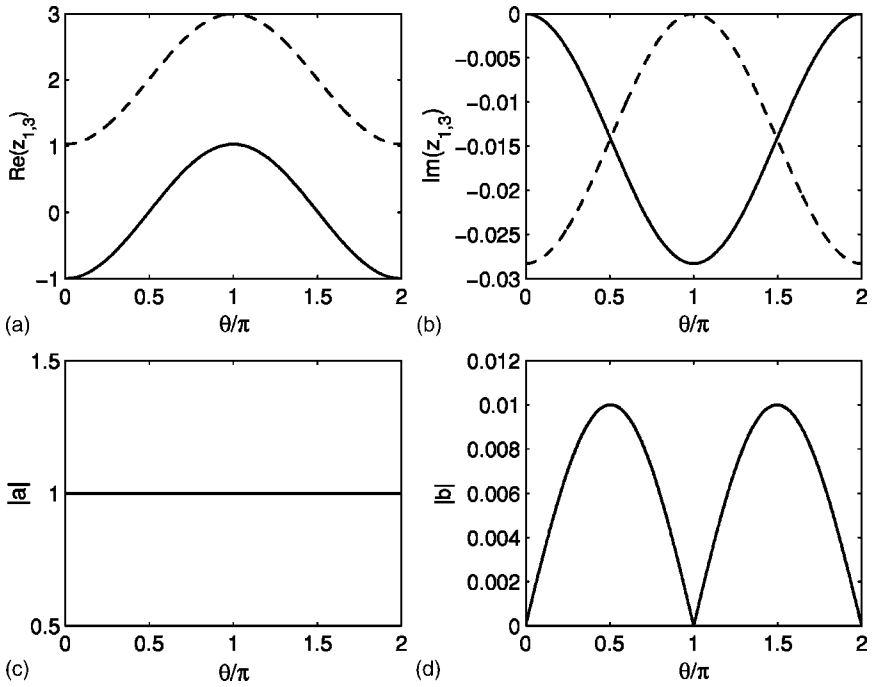

FIG. 15. The evolution of the eigenvalues $z_{1,3}$ (a, b), and of the components a and b of the eigenvectors (c, d) of the effective Hamiltonian for the circular encircling of the DP given by Eq. (19). $v=0.2$, $\varepsilon_1=1$, $\epsilon(L)=2-L/5$, $E=\sqrt{2}$, $r=1$. The eigenvalues and eigenvectors are restored after every cycle.

of the bumps that occurs in the amplitudes of the wave functions (Fig. 16) is a typical interference effect. It is caused by the fact that there are altogether three states two of which interfere. The phases of the eigenfunctions of H_{eff} are restored after every cycle of circular or elliptical encircling when $v\neq 0$ (not shown). A Berry phase does not appear.

The difference between the two cases with $v=0$ and $v\neq 0$ can be seen best when $u\to 0$ is passed on the path of encircling. When $v=0$, the phases of both wave functions are changed after one encircling, i.e., the Berry phase appears. When however $v\neq 0$, such a phase change does not occur since the system has the additional freedom to change the widths of the states, see Figs. 15 and 16. The Berry phase vanishes therefore when $v\neq 0$ but the widths depend strongly on the angle: in every cycle, the widths of the two states are twice equal to one another and differ twice by the maximum possible value from one another. The last case corresponds to width bifurcation appearing when $u=0$ (and $v/u\to\infty$) is passed. The width bifurcation seen at $u=0$ shows that the DP is unfolded into two BPCPs, with different chirality when $v\neq 0$ (and $v/u\to\infty$). Encircling the DP does therefore not influence the phases of the eigenvectors of the effective Hamiltonian. This result corresponds to the mapping shown in Fig. 7.

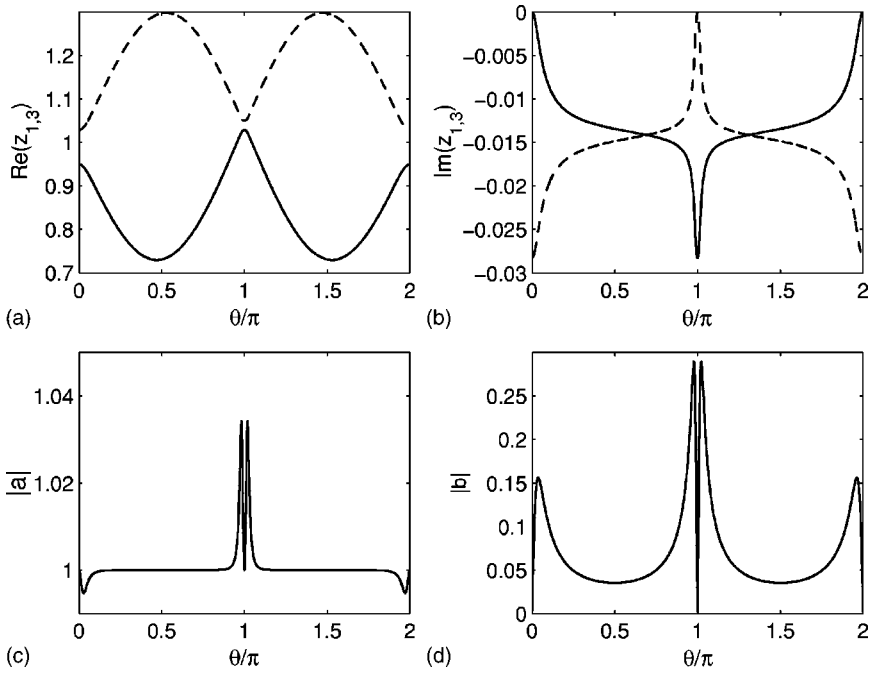

FIG. 16. The same as Fig. 15, but the BP is encircled by the elliptic path $L=5+0.25\cos\theta$, $u=0.1\sin\theta$ as in Figs. 13 and 14. The eigenvalues and eigenvectors are restored after every cycle.

VII. CONCLUDING REMARKS

In the double QD considered by us, the eigenvalues of two states coalesce at the DPs in the real plane as well as at the BPCP. At the DPs, the interaction u vanishes and the system decomposes into three independent parts. At the BPCP, however, the system as a whole is well defined with nonvanishing interaction u between the two single dots and the internal wire and a nonvanishing coupling v of the double dot to the two attached leads. The BPCP are physically relevant.

The avoided crossings of discrete states can analytically continued to those of resonance states [8]. The DPs characterize true crossings of discrete states while the BPCP are related to true crossings of resonance states. Although both, DPs and BPCP, are related to avoided level crossings, they are different from one another. The DPs are within the avoided crossing scenario of discrete states. The BPCP, however, are singular points that separate the avoided level crossing scenario from that with different Riemann sheets and without level crossings.

When $F=0$, the eigenvalues z_1 and z_3 of $H_{\rm eff}$ coalesce and the eigenvectors $|1)$ and $|3)$ have some nontrivial properties [10]. According to (9) [10] and Figs. 4–6, the components of the (complex) eigenvectors $|1)$ and $|3)$ diverge when $F\to 0$ (for the open quantum system with $v\neq 0$ and $u\neq 0$). The biorthogonality relation $(z_k|z_l)$ is therefore fulfilled also in approaching $F=0$, since the difference between two infinitely large numbers may be 0 or 1. Further [10]:

$$|1) = \pm i|3), \quad \text{when } F=\xi^2=0. \tag{21}$$

The last relation does not mean that the two wave functions $|1)$ and $|3)$ are linearly dependent at the BPCP since their components are infinitely large at this singular point. It holds not only for the special system considered here. It holds generally for the eigenvectors of a nonhermitian Hamilton operator [6,8,21] and expresses nonlinear effects in the open quantum system, see later. Another concrete example are the eigenfunctions of the effective Hamiltonian that describes atoms under the influence of a laser field [15]. The function space can therefore *not* be considered as incomplete at the BPCP. At these points, different Riemann sheets evolve which are caused by the width bifurcation taking place at the BPCP.

The relation (21) means that the states at the BPCP are chiral states. Let $|1)\to \pm i|3)$ and $|3)\to \mp i|1)$ according to (21) when the BPCP is approached. Then the wave functions at the BPCP may be written, e.g., as $\psi_+=\frac{1}{2}\{|1)\pm i|3)\}$; $\psi_-=\frac{1}{2}\{|3)\mp i|1)\}$. The $\psi_\pm$ are wave functions of chiral states, where the sign $\pm$ determines the chirality.

Another difference between BPCP and DPs is related to nonlinear effects caused by the overlapping of resonance states. In order to show this, let us rewrite the effective Hamiltonian (2) as

$$H_{\rm eff} = H^0_{\rm eff} + W = H^0_{\rm eff} + \begin{pmatrix} 0 & 0 & f \\ 0 & 0 & 0 \\ f & 0 & 0 \end{pmatrix}, \tag{22}$$

where $H^0_{\rm eff}$ is the diagonal part of $H_{\rm eff}$ and the nondiagonal matrix elements f given by (10) [10] describe the coupling between the two resonance states 1 and 3 due to their overlapping. Then, the Schrödinger equation with the Hamiltonian $H^0_{\rm eff}$ reads

$$[H^0_{\rm eff} - z_l]|l) = -\begin{pmatrix} 0 & 0 & f \\ 0 & 0 & 0 \\ f & 0 & 0 \end{pmatrix}|l) \equiv -W|l). \tag{23}$$

The eigenfunctions of $H_{\rm eff}$, given in Eq. (9) [10], are biorthogonal, $H_{\rm eff}|k)=z_k|k)$ with $(k|l)\equiv\langle k^*|l\rangle=\delta_{k,l}$. From these relations follows:

$$\langle k|k\rangle = \mathrm{Re}\langle k|k\rangle, \quad A_k \equiv \langle k|k\rangle \geqslant 1,$$

$$\langle k|l\rangle = i\,\mathrm{Im}\langle k|l\rangle = -\langle l|k\rangle, \quad |B^l_k| \equiv |\langle k|l\rangle| \geqslant 0,\ l\neq k. \tag{24}$$

Using these equations, the right-hand side (rhs) of Eq. (23) reads [6,8]:

$$W|l) = W|l\rangle = \sum_{k=1,3}\langle k|W|l\rangle \sum_{m=1,3}\langle k|m\rangle|m\rangle$$
$$= W^{1l}(A|1\rangle + iB|3\rangle) + W^{3l}(A|3\rangle - iB|1\rangle) \tag{25}$$

with $W^{kl}\equiv\langle k|W|l\rangle$, $k=1,3$. This relation gives $|l)\to\pm i|j)$, $l\neq j$, in approaching the BPCP due to $A_l=\to\infty$, $B^j_l=\to\infty$ what agrees with (21). Furthermore, we see that nonlinear terms, caused by the interaction f, appear in the Schrödinger Eq. (23) as soon as $A\neq 1$ and $B\neq 0$, i.e., as soon as the resonance states overlap. This means, nonlinear terms in the Schrödinger equation appear due to the overlapping of resonance states. They are large in the neighborhood of BPCP. An analogous effect does not occur in the neighborhood of DPs.

The nonlinear effects can be seen in the line shape of resonances. Knowing the eigenvalues and eigenfunctions of $H_{\rm eff}$, the S matrix can be written down. When two eigenvalues coalesce, it reads [9,34]:

$$S = 1 + 4i\frac{\mathrm{Im}(z_d)}{E-z_d} - 4\frac{\mathrm{Im}(z_d)^2}{(E-z_d)^2}, \tag{26}$$

where $z_d\equiv z_1=z_3$ and the smooth background is neglected. Equation (26) shows that the nonlinear terms in (23) influence directly the line shape of overlapping resonances. The extreme case Eq. (26) occurs when the eigenvalues of two resonance states coalesce at the energy $E=E_k=\mathrm{Re}(z_k)|_{E=E_k}$, $k=1,3$, i.e., when the S matrix has a double pole at $E=E_1=E_3$ [30]. The interference between the two resonance states 1 and 3 leads to an interference minimum (zero) at the energy $E=\mathrm{Re}(z_d)$. At this energy, an isolated resonance of Breit-Wigner shape has its maximum (peak) since there are no neighbored resonances and the third term on the rhs of (26) does not appear. Examples for line shapes with overlapping resonances are considered in, e.g., Refs. [6,15,34].

The results represented in Figs. 15 and 16 need to be compared with those obtained in Ref. [24] for the phase obtained from encircling the crossing point of Gamow states. This phase consists of two parts: one part is the well-known expression for the Berry phase of two interfering bound

states that are adiabatically transported in parameter space around the point of the accidental degeneracy of two eigenvalues. The other part is proportional to the width of the state and vanishes when the width vanishes.

The difference between this result and those represented in the present paper consists, above all, in the difference between a Gamow state and a discrete state embedded in the continuum. Every Gamow state has its own continuum part. Embedding of the Gamow states into a common continuum of scattering states [35] is not considered in Ref. [24].

In contrast to this, the different resonance states considered by us in the present paper are discrete states embedded in one and the same environment (common continuum of scattering wave functions). The function space is enlarged, indeed, in our calculations by opening the system: it consists not only of discrete states but contains also the common scattering states (for details see Refs. [6,16]). The wave functions of discrete states and scattering states form each a subspace of the total function space according to the Feshbach unified theory of nuclear reactions [11]. The discrete states characteristic of one of the subspaces, pass into resonance states when they are embedded in the other subspace, i.e., the common continuum of scattering states [12]. The wave functions of the resonance states contain contributions from both the discrete states and the common continuous states [6,16]. When the system is opened at the DP and encircled, one of the two resonance states passes back, with $u \to 0$, into the function space of discrete states by loosing its width while the other one becomes a short-lived resonance state.

Thus, there is no contradiction of our results to those obtained in Ref. [24]. Obviously, the Berry phase appears always when the considered states are not embedded into a common continuum and do not interact via the environment. In this sense, the Berry phase is related to the incompleteness of the function space. The Berry phase vanishes by embedding the system into the common continuum of scattering states due to which the system turns over into a subsystem and the discrete states become resonance states [12], see Sec. VI.

The results discussed in the present paper coincide with the unfolding of the DP into two different BPCP when the system is opened, as suggested in Ref. [21]. The two BPCP appear due to the two different signs of the coupling strength v between system and environment and have, as shown in Sec. III, different chirality. The difference between the encircling of the DP at $v=0$ and the same encircling, but $v \neq 0$, is that the left and right wave functions are equal to one another in the first case while they are different from one another in the second case, see Sec. VI. As a consequence, the Berry phase appears in the first case and not in the second case where the function space is enlarged by including the continuum of scattering wave functions. Moreover, it has been shown in Fig. 7 that the encircling of a DP does not cause a geometric phase in the open system.

In the avoided level crossing scenario, the phases of the wave functions evolve as a function of v. This means that the real and imaginary parts of the eigenfunctions of the Hamiltonian H_{eff} decouple to a great deal. Both parts evolve more or less independently from one another up to the BPCP. As has been shown in Ref. [10], this fact influences physical observables as, e.g., the transmission through a double QD.

All the results discussed in this paper show that the BPCP are physically meaningful since they influence observables. They are responsible for the transition from one scenario to another one that both are qualitatively different from one another: one scenario is characterized by level repulsion and similar decay widths of the states while the other one results from width bifurcation and is accompanied by some level clustering [6,10]. The DPs do not have such a physical meaning. The different nature of DPs and BPCP corresponds with the fact that the topological structure of DPs and BPCP is different from one another (Figs. 7 and 8).

ACKNOWLEDGMENTS

We thank the Max-Planck-Institut für Physik komplexer Systeme for hospitality. This work has been supported by RFBR Grant Nos. 05-02-97713 and 05-02-17248.

[1] T. Kato, *Perturbation Theory of Linear Operators*, 2nd ed. (Springer, Berlin, 1980).
[2] M. V. Berry, Proc. R. Soc. London, Ser. A **392**, 45 (1984).
[3] M. V. Berry and M. Wilkinson, Proc. R. Soc. London, Ser. A **392**, 15 (1984).
[4] R. Y. Chiao and Y. S. Wu, Phys. Rev. Lett. **57**, 933 (1986); A. Tomita and R. Y. Chiao, *ibid.* **57**, 937 (1986); R. S. Nikam and P. Ring, *ibid.* **58**, 980 (1987); R. Tycko, *ibid.* **58**, 2281 (1987); T. Bitter and D. Dubbers, *ibid.* **59**, 251 (1987); S. Clough, G. J. Barker, K. J. Abed, and A. J. Horsewill, *ibid.* **60**, 136 (1988); R. Bhandari and J. Samuel, *ibid.* **60**, 1211 (1988); R. Y. Chiao, A. Antaramian, K. M. Ganga, H. Jiao, and S. R. Wilkinson, *ibid.* **60**, 1214 (1988); D. Suter, K. T. Mueller, and A. Pines, *ibid.* **60**, 1218 (1988).
[5] H. M. Lauber, P. Weidenhammer, and D. Dubbers, Phys. Rev. Lett. **72**, 1004 (1994).
[6] J. Okołowicz, M. Płoszajczak, and I. Rotter, Phys. Rep. **374**, 271 (2003).
[7] N. Moiseyev, Phys. Rep. **302**, 211 (1998).
[8] I. Rotter, Phys. Rev. E **64**, 036213 (2001).
[9] I. Rotter, Phys. Rev. E **68**, 016211 (2003).
[10] I. Rotter and A. F. Sadreev, Phys. Rev. E **69**, 066201 (2004).
[11] H. Feshbach, Ann. Phys. (N.Y.) **5**, 357 (1958); **19**, 287 (1962).
[12] Sometimes, the widths of the resonance states vanish. This may happen due to selection rules or due to the resonance trapping phenomenon at certain values of the tuning parameter [6,15,27]. The selection rules do never hold with 100% accuracy because of higher-order contributions that become important as soon as the main contribution is forbidden. The resonance trapping phenomenon may cause a vanishing (or nearly vanishing minimum) value of the width of a certain resonance

state at a certain value of the tuning parameter. The width of this state for neighboring values of the tuning parameter is however nonvanishing, in any case. Concrete examples are considered in atoms [15] and in double quantum dots [27]. It is resonable therefore to generalize the term resonance state and to call *all* states that are embedded in the continuum, "resonance states" independently of the value of their widths.

[13] M. Müller, F. M. Dittes, W. Iskra, and I. Rotter, Phys. Rev. E **52**, 5961 (1995).

[14] E. Persson, T. Gorin, and I. Rotter, Phys. Rev. E **54**, 3339 (1996).

[15] A. I. Magunov, I. Rotter, and S. I. Strakhova, J. Phys. B **32**, 1669 (1999); **34**, 29 (2001).

[16] I. Rotter, Rep. Prog. Phys. **54**, 635 (1991).

[17] W. D. Heiss, M. Müller, and I. Rotter, Phys. Rev. E **58**, 2894 (1998); W. D. Heiss, Eur. Phys. J. D **7**, 1 (1999); Phys. Rev. E **61**, 929 (2000).

[18] C. Dembowski, H. D. Gräf, H. L. Harney, A. Heine, W. D. Heiss, H. Rehfeld, and A. Richter, Phys. Rev. Lett. **86**, 787 (2001).

[19] C. Dembowski, B. Dietz, H. D. Gräf, H. L. Harney, A. Heine, W. D. Heiss, and A. Richter, Phys. Rev. Lett. **90**, 034101 (2003).

[20] C. Dembowski, B. Dietz, H. D. Gräf, H. L. Harney, A. Heine, W. D. Heiss, and A. Richter, Phys. Rev. E **69**, 056216 (2004).

[21] F. Keck, H. J. Korsch, and S. Mossmann, J. Phys. A **36**, 2125 (2003).

[22] In Refs. [17–21,23], the BPCP are called "exceptional points" although the function space at these singular points is *not* incomplete. Instead, the phases of the wave functions of the two crossing states are undetermined, see Figs. 4, 5, and 6, the discussion on Gamow states in Sec. VII, and Refs. [6,10]. The incompleteness of the Hilbert space is characteristic of exceptional points [1]. The chirality of the states at the singular points is determined by the sign in Eq. (21).

[23] W. D. Heiss and H. L. Harney, Eur. Phys. J. D **17**, 149 (2001).

[24] A. Mondragon and E. Hernanández, J. Phys. A **26**, 5595 (1993); **29**, 2567 (1996); E. Hernández, A. Jáuregui, and A. Mondragon, *ibid.* **33**, 4507 (2000); Phys. Rev. A **67**, 022721 (2003).

[25] I. Rotter, Phys. Rev. E **65**, 026217 (2002); **67**, 026204 (2003).

[26] A. F. Sadreev and I. Rotter, J. Phys. A **36**, 11413 (2003).

[27] I. Rotter and A. F. Sadreev, Phys. Rev. E (to be published), e-print cond-mat/0403184.

[28] C. Mahaux and H. A. Weidenmüller, *Shell Model Approach in Nuclear Reactions* (Amsterdam, North Holland, 1969).

[29] F. M. Dittes, Phys. Rep. **339**, 215 (2000).

[30] The fixed-point solutions are defined [16,6] by $E_k = \mathrm{Re}(z_k)|_{E=E_k}$ and $\Gamma_k = -2\mathrm{Im}(z_k)|_{E=E_k}$. Since only real E are considered, this definition is not related to any singularity. The singularities (BPCP) that appear when two eigenvalues of H_{eff} coalesce are therefore of first order. For narrow resonances, the fixed-point solutions coincide with a pole of the S matrix.

[31] E. Persson, I. Rotter, H. J. Stöckmann, and M. Barth, Phys. Rev. Lett. **85**, 2478 (2000); H. J. Stöckmann, E. Persson, Y. H. Kim, M. Barth, U. Kuhl, and I. Rotter, Phys. Rev. E **65**, 066211 (2002).

[32] S. Rotter, F. Libisch, J. Burgdörfer, U. Kuhl, and H. J. Stöckmann, Phys. Rev. E **69**, 046208 (2004).

[33] F. Pistolesi and N. Manini, Phys. Rev. Lett. **85**, 1585 (2000); N. Manini and F. Pistolesi, *ibid.* **85**, 3067 (2000).

[34] A. I. Magunov, I. Rotter, and S. I. Strakhova, Phys. Rev. B **68**, 245305 (2003).

[35] A method alternative to the continuum shell model for the description of unstable nuclear states is the Gamow shell model ("shell model in the Berggren basis"), see the recent review [6] and references therein. In the *continuum shell model*, the shell model states are constructed by means of bound single-particle states. The discrete shell model states are embedded in the continuum, i. e., the completeness relation of the wave functions contains both the discrete shell model states (Q subspace) as well as the nonresonant continuum (P subspace). Although the *Gamow shell model* is based on the unbound Gamow states (together with the bound single-particle states), the Berggren completeness relation of the wave functions contains additionally the nonresonant continuum. That means, in spite of taking into account the finite lifetime of the unbound single-particle states, the states of the Gamow shell model are also embedded in the common continuum.